Aerodynamic Shattering of Ice Crystals in Hypersonic Flight

Girard A. Simons*
Physical Sciences Inc., Woburn, Mass.

A theoretical study of ice crystal/shock-layer interaction has been carried out in order to assess the relative kinetic energy of an ice crystal upon impact with a hypersonic vehicle. A dynamic fracture criterion has been developed which predicts the size of the ice crystal fragments formed at the vehicle bow shock. An analysis of the ice crystal breakup predicts that the outer fragments continue to shatter and prevent the shock-layer gas from penetrating the fragment cloud. Thus, the fragment cloud may be treated as a distinct deformable fluid. The reduced impact velocity due to lateral spreading of the fragment cloud may be determined from existing work on raindrop deformation in hypersonic shock layers.

I. Introduction

As a supersonic or hypersonic vehicle passes through a real atmosphere, vehicle erosion may occur because of its encounter with relatively large clouds of dust, rain, and ice. The vehicle shock layer may offer some shielding of the vehicle from the erosive material. Hence, the interaction of the erosive material with the shock layer has become an important problem. A great deal of attention has previously been given to the problems of dust[1] and rain,[2-11] but not until recently has significant effort been devoted to the interaction of ice crystals with the shock layer. Wu[12] has studied the melting and vaporization of an ice crystal in a hypersonic shock layer and demonstrated a significant reduction in particle size and impact velocity for ice crystals initially of the order of 10-μ diameter. Larger crystals were relatively unaffected by melting and vaporization. In the same report, Teare[12] demonstrated that ice crystals may shatter at the vehicle bow shock. This introduces the possibility that the fractured ice crystal or "fragment cloud" may deform as it passes through the vehicle shock layer. This deformation will be lateral to the relative gas velocity and will tend to increase the drag area of the fragment cloud. Hence, the velocity of the fragment cloud will decrease more rapidly than that of a rigid particle, and the velocity with which the fragment cloud impacts the vehicle may be significantly lower than that with which a "rigid" ice crystal would impact the vehicle.

To study this phenomenon, we examine the interaction of the ice crystal with the shock layer over three distinct time scales: fracture, breakup, and deformation. The first time scale is the time required for a stress wave to propagate across the ice crystal and generate multiple fractures. Analysis of this event requires the development of a dynamic fracture criterion. Such a criterion is developed in Sec. II. We consider a monochromatic stress wave and determine an appropriate monochromatic yield criterion. We then assert that a dynamic yield criterion may be obtained by Fourier expanding the applied load and applying the monochromatic yield criterion to each wave. Using this basic hypothesis, we determine the maximum size (ℓ) of the ice crystal fragments allowed by the highest mode that can just fracture the ice crystal. The behavior of a cloud or "gas" of such fragments is needed to describe the motion of the fractured ice crystal through the vehicle shock layer.

Received Jan. 7, 1976; revision received Aug. 2, 1976. Research jointly sponsored by the Space and Missile Systems Organization and the Air Force Office of Scientific Research (AFSC), United States Air Force, under Contract F44620-74-C-0022.

Index categories: Multiphase Flows; Structural Dynamic Analysis; Hypervelocity Impact.

*Principal Scientist. Member AIAA.

As the fractured ice crystal passes through the vehicle shock layer, it will break up and deform by the action of the shock-layer gas. The time scale for the gas to penetrate the fragment cloud is short compared to the time required for the fragment to respond dynamically to the gas. The latter time scale is the deformation time and, on a time scale small with respect to the cloud deformation time, ice crystal breakup must be assessed in order to determine the appropriate model for the fragment cloud. That is, does the fragment cloud behave as a separate gas, a two-phase flow, or as a fluidized bed? This question is addressed in Sec. III. Using the dynamic shattering model, it is shown that the outer fragments continue to fracture and prevent the shock layer gas from penetrating the fragment cloud. Thus, the fragment cloud may be treated as a separate incompressible gas without surface tension. This conclusion is a consequence of the dynamic fracture criterion which itself is subject to experimental confirmation. However, the dynamics of ice crystal breakup are insensitive to the actual shattering process and this basic conclusion is only weakly dependent on the actual dynamic shattering criterion.

The dynamics of the fragment cloud have been modeled and published separately.[13] The Reinecke-Waldman model for liquid drop deformation is extended to include a time-dependent relative wind. The lateral spreading of the fragment cloud may significantly reduce the impact velocity of the ice crystal on the hypersonic vehicle.

II. Initial Fracture of the Ice Crystal

A. Dynamic Fracture Criterion

A schematic of an ice crystal entering a hypersonic shock layer is given in Fig. 1. The ice crystal enters the vehicle shock layer with velocity U_∞, finds itself moving with supersonic velocity relative to the shock layer gas, and thereby generates its own bow shock or crystal shock. The resulting pressure on the ice crystal is an impulsively applied load which may be one to two orders of magnitude in excess of the static yield stress. Hence, a consistent dynamic yield criterion must be established in order to analyze the shattering problem. First, we define the two times relevant to dynamic loads. τ_T is the transient time for application of the load and τ_R is the response time or the time required for the entire specimen of length L to know a load has been applied. Clearly, $\tau_R = L/a_0$, where a_0 is the speed of sound in the specimen.

By definition, static loading occurs when $\tau_T \gg \tau_R$ and the static yield stress (σ_s) is the appropriate measure of the maximum load which the specimen can tolerate without plastic deformation or failure. Clearly, when $\tau_T \ll \tau_R$, a dynamic yield stress (σ_D) is a necessary measure of failure.

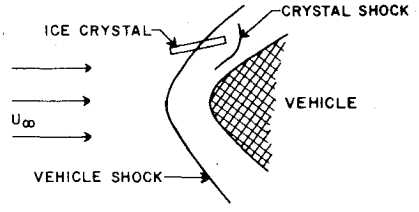

Fig. 1 Ice crystal/shock-wave interaction.

When $\tau_T = O(\tau_R)$ we assert that $\sigma_D = O(\sigma_s)$. This assertion is verified by impact experiments.[14] These experiments demonstrate that when a projectile undergoes a collision with a "rigid" target, the projectile appears to have a dynamic yield stress of the order twice the static yield stress. Under this loading situation, the projectile is loaded for two wave passage times. Hence, we have empirical evidence that $\sigma_D = O(\sigma_s)$ when $\tau_T = O(\tau_R)$.

Another example of a situation where $\tau_T = \tau_R$ is a monochromatic stress wave. Let X_x be the longitudinal stress (tension or compression) in a stress wave

$$X_x = A_k \sin(\pi k a_0 t) \cos(\pi k x)$$

For an element of length $1/k$, $\tau_R = \tau_T = (1/ka_0)$. Therefore, failure occurs when $A_k = O(\sigma_s)$. An alternate way of looking at the stress wave is in terms of the particle velocities U_x. The momentum equation

$$\rho \frac{\partial U_x}{\partial t} = X_x$$

yields

$$U_x = \frac{a_0 A_k}{E} \cos(\pi k a_0 t) \sin(\pi k x)$$

where E is Young's Modulus relating stress σ to strain e ($\sigma = Ee$, and $a_0 = \sqrt{E/\rho}$). If we interpret U_x as a series of elements of length $1/k$ colliding with velocity $a_0 A_k/E$, then impact theory[14] indicates that failure occurs when the impact velocity exceeds $O(e_s a_0)$. Since $\sigma_s = Ee_s$, this criterion reduces to $A_k = O(\sigma_s)$.

Having developed a rational argument for applying a static yield criterion to the monochromatic stress wave, we now make the following bold hypothesis which, though plausible, can be justified only if the subsequent conclusions agree with experiment.

Hypothesis: Dynamic yield stress may be obtained by Fourier expanding the applied load and applying the monochromatic yield criterion to each wave. Failure occurs when $A_k = Q\sigma_s$ where Q is $O(1)$ and is to be determined by applying this technique to explain empirical observations.

Before utilizing this hypothesis to examine the catastrophic failure of an excessively overloaded material, the physical implications of the failure model will be discussed. The dynamic yield stress must be a function of both the load transients and the material properties. These effects will enter the analysis through the Fourier coefficient A_k. Since all of the information which appears in the dynamic equations and boundary conditions will enter into A_k, the dynamic yield stress will be a function of Young's Modulus E, the material density ρ, the speed of sound $\sqrt{E/\rho}$, all knowledge of the load transients, the static yield stress σ_s, and the parameter Q. To describe the meaning of Q, recall that the impact experiments[14] yield empirical evidence that $\sigma_D = O(\sigma_s)$ when $\tau_T = O(\tau_R)$. The monochromatic yield criterion is a formulation of this observation and the parameter Q is introduced to reflect the ratio between σ_D and σ_s in the limit $\tau_T = O(\tau_R)$. More specifically, Q is the ratio of the dynamic yield stress under a sinusoidal load to the static yield stress. One initially would expect that Q is a function of the rate of strain $\dot{e}$, since we use a sinusoidal load as a reference condition. Rate of strain effects will be discussed in Sec. IIC where the stress tensor is extended to include $\dot{e}$. The rate of strain then may influence the dynamic yield stress through the Fourier coefficient A_k, but the parameter Q must be independent of $\dot{e}$ because the sinusoidal reference condition is strictly valid only when $\dot{e}$ is zero. Hence, Q must be evaluated when $\dot{e}$ is finite but negligible. The value of Q will be a material constant, as in the case of the impact experiments. The material property reflected by this parameter is the plastic nature of the material. Hence, plasticity can enter the present theory only by allowing Q to be a material constant. For the purpose of this paper, we shall restrict the analysis to brittle materials and proceed under the assertion that Q is a universal constant.

Having developed a theory for the catastrophic failure of a brittle material, we now shall apply it to the problems of fracture and shattering. To expedite the mathematics, we shall assume that a standing wave forms in the specimen before fracture occurs. Although this approximation may have to be relaxed in the light of empirical information, it should be emphasized that the standing wave approximation is distinct from the fracture hypothesis and that failure of this approximation need not imply the failure of the fracture hypothesis.

B. One-Dimensional Fracture

Let us first examine the present theory by applying it to the problem of a one-dimensional slab of thickness b that is loaded impulsively on one side with pressure P_s for time τ_D. The load is removed impulsively at the end of that time interval ($\tau_D \ll b/a_0$). A schematic of the loading and unloading waves in (x,t) coordinates is given in Fig. 2. If we stand at some position x between $a_0\tau_D/2$ and $b - a_0\tau_D/2$, the time-dependent force on an element is shown in Fig. 3. The Fourier expansion of X_x is given by

$$X_x = \sum_n \frac{4P_s}{n\pi} \sin\left(\frac{n\pi a_0 \tau_D}{2b}\right) \sin\left(\frac{n\,\pi a_0 t}{b}\right) \sin\left(\frac{n\pi x}{b}\right)$$

The dynamic fracture criterion indicates that the primary mode ($n = 1$) will fracture the specimen if

$$\frac{4P_s}{\pi} \sin\left(\frac{\pi a_0\ \tau_D}{2b}\right) \approx \frac{2\ P_s a_0 \tau_D}{b} > Q\sigma_s$$

or

$$P_s > \left(\frac{Qb}{2\ a_0 \tau_D}\right)\sigma_s$$

Hence, the dynamic yield stress σ_D is given by

$$\sigma_D = \left(\frac{Qb}{2\ a_0 \tau_D}\right)\sigma_s \qquad \text{for } \tau_D \ll b/a_0$$

and illustrates that σ_D is inversely proportional to τ_D and indeed is in excess of σ_s provided that Q is of order unity.

To determine the value of Q, let us again take a one-dimensional slab and impulsively load it in tension (T) for all time. The wave diagram is illustrated in Fig. 4 and the pressure-time history is shown in Fig. 5. The corresponding Fourier series representation of the dynamic load is given by

$$X_x = T + \sum_n \frac{2T}{n\pi}\left(\cos n\pi - 1\right) \sin\left(\frac{n\pi x}{b}\right) \cos\left(\frac{n\pi a_0 t}{b}\right)$$

An impulsively applied load creates twice the strain of a slowly applied load.[15] Thus, the impulsive load will fracture

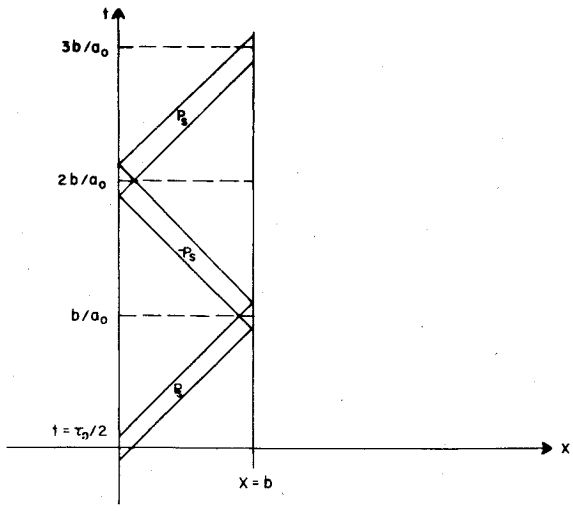

Fig. 2 Wave diagram of impulsive short term load.

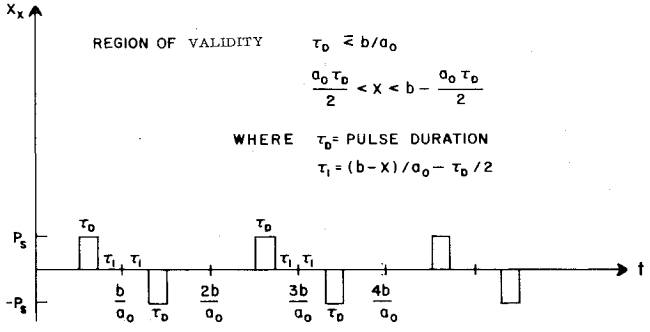

Fig. 3 Pressure "trace" for impulsive short term load.

the specimen when T is only $\sigma_s/2$. Equating the amplitude of the $n=1$ mode of the preceding expansion to $Q\sigma_s$, we determine

$$Q_{1D} \equiv 2/\pi \tag{1}$$

Note that we have obtained Q by comparing the amplitude of standing waves. Any subsequent use of the value of Q must be made with standing waves. A completely consistent approach could be developed using traveling waves but the values of Q would differ by a factor of 2.

Having developed a criterion for fracture of a dynamically loaded specimen, let us now examine shattering. Consider a one-dimensional slab impulsively loaded on one side and held constant for all time. This is the one-dimensional analogue of the ice crystal loading at the bow shock of a hypersonic vehicle. The Fourier expansion of the dynamic load is expressed as

$$X_x = \sum_n -\frac{2P_s}{n\pi}\cos\left(\frac{n\pi a_0 t}{b}\right)\sin\left(\frac{n\pi x}{b}\right) + P_s\left(1-\frac{x}{b}\right)$$

Suppose $P_s \gg \sigma_s$. Then, not only can the $n=1$ mode fracture the specimen, but the $n=2$ mode can break those fragments and so on up to the critical value of $n(n_c)$ where the nth mode is just strong enough to fracture the specimen. This value of n is determined by

$$2P_s/n_c\pi = Q\sigma_s$$

or

$$n_c = P_s/\sigma_s$$

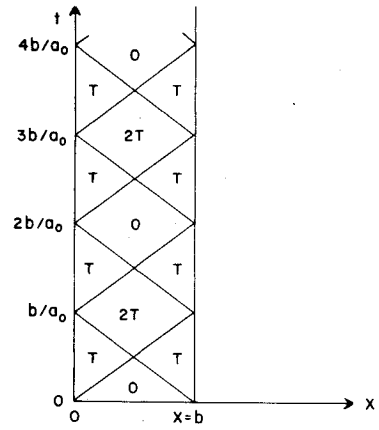

Fig. 4 Wave diagram for impulsive load in tension.

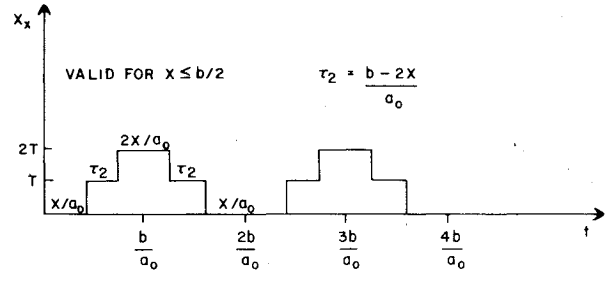

Fig. 5 Pressure "trace" for impulsive load in tension.

and the corresponding size of the fragments ℓ of the n_c mode is given by

$$\ell = b/n_c = (\sigma_s/P_s)\,b$$

These are the largest fragments that can survive the applied pressure P_s. Smaller fragments can exist because of the shattering by other modes. That is, the n_cth mode fractures the specimen at values of x/b equal to

$$\frac{x}{b} = \frac{1}{2n_c}, \frac{3}{2n_c}, \frac{5}{2n_c}, \frac{7}{2n_c} \cdots \frac{2n_c-1}{2n_c}$$

The $n_c - 1$ mode fractures the specimen at

$$\frac{x}{b} = \frac{1}{2(n_c-1)}, \frac{3}{2(n_c-1)}, \frac{5}{2(n_c-1)}, \frac{7}{2(n_c-1)} \cdots \frac{2(n_c-1)-1}{2(n_c-1)}$$

The largest fragment is then

$$\frac{\Delta x}{b} = \frac{3}{2n_c} - \frac{1}{2n_c} = \frac{1}{n_c}$$

whereas the smallest is

$$\frac{\Delta x}{b} = \frac{1}{2(n_c-1)} - \frac{1}{2n_c} \approx \frac{1}{2n_c^2}$$

Therefore, for one-dimensional shattering, we have determined that the fragment sizes range from the smallest

$$\ell_{\min} = \tfrac{1}{2}(\sigma_s/P_s)^2 b$$

to the largest

$$\ell_{\max} = (\sigma_s/P_s)\,b \tag{2}$$

Since the ice crystal erosion problem is dominated by the large crystals, we shall study the two-dimensional and three-dimensional shattering problems with the understanding that the characteristic fragment size refers to the largest fragments, and that smaller fragments can exist.

C. High-Frequency Limitations

The results of Sec. II B place no upper limit on the frequency of the fracturing wave or, equivalently, place no lower limit on the size of the shattered fragments. It is well known[16] that the minimum wavelength that can exist in a solid is of the order of the lattice spacing s and the maximum frequency is the phonon frequency ω_p

$$\omega_p \approx a_0/s$$

where a_0 is the speed of sound in the specimen. These concepts may be included in the shattering analysis by adding some "inertia" to the stress tensor. Assuming

$$\sigma = E(e+\beta\,\dot{e})$$

where $\dot{e}$ is $\partial e/\partial t$ and both E and β are constants, the momentum equation becomes

$$\rho\frac{\partial^2 U}{\partial t^2} = \frac{\partial \sigma}{\partial x} = E\frac{\partial^2 U}{\partial x^2} + E\beta\frac{\partial^3 U}{\partial t \partial x^2}$$

Solving the initial value problem,

$$U(x,t) = \sin\left(\frac{2\pi x}{\lambda}\right) e^{-\omega t}$$

for λ real and ω complex, we see that propagation cannot exist above the frequency $2/\beta$ or below the wavelength $\pi a_0 \beta$. Hence, it follows that

$$\beta \approx 1/\omega_p \approx s/a_0$$

Solving the boundary value problem,

$$U(x,t) = e^{-x/\delta_e} e^{i(\omega t - 2\pi x/\lambda)}$$

for ω, λ, and the decay depth δ_e all real, we obtain

$$\delta_e \approx 2a_0/\omega^2\beta \approx {a_0}^2/s\omega^2$$

where δ_e approaches s as ω approaches ω_p.

For an applied load of arbitrary frequency ω, caution must be taken to insure that $\delta_e > b$ before using the proposed dynamic yield criterion since it omits skin depth effects. For an impulsively loaded specimen of length b, the frequency corresponding to the nth mode is

$$\omega \approx n a_0/b$$

Validity of the shattering analysis requires

$$\delta_e > b$$

or

$$b > n^2 s$$

or

$$\ell_{\max} > ns$$

and

$$\ell_{\min} > s$$

Thus, the ice crystal shattering analysis is valid down to fragment sizes of the order of s. High-frequency effects do not influence the shattering by an impulsively applied load but may become important for high-frequency loads and large test specimens.

D. Two-Dimensional Fracture

The one-dimensional shattering analysis is readily extended to two dimensions by expanding the applied load into a double Fourier series. Suppose we have a two-dimensional ice crystal with pressure P_s impulsively applied at one end. Assuming that the shear modulus is negligible, the applied pressure may be expanded as a square wave over the lateral dimension a of the ice crystal

$$P_s(y) = \frac{2P_s}{\pi}\sum_m \left(\frac{1-\cos m\pi}{m}\right)\sin\left(\frac{m\pi y}{a}\right)$$

The one-dimensional plane wave solution was given by

$$X_x = \sum_n \frac{-2P_s(y)}{n\pi}\cos\left(\frac{n\pi a_0 t}{b}\right)\sin\left(\frac{n\pi x}{b}\right)$$

where a_0 was $\sqrt{E/\rho}$ and $P_s(y)$ was constant. Thus, the plane wave representation of an end loaded two-dimensional ice crystal is given by

$$X_x = \sum_m \sum_n \frac{-4P_s(1-\cos m\pi)}{m\,n\pi^2}\sin\left(\frac{m\pi y}{a}\right)\sin\left(\frac{n\pi x}{b}\right) \cdot\cos\left(\frac{n\pi a_0 t}{b}\right)$$

or, in standing wave form

$$X_x = \sum_m \sum_n \frac{-2P_s(1-\cos m\pi)}{n\,m\pi^2}\cos\left(\frac{n\pi a_0 t}{b}\right) \cdot\left[\cos\left\{\frac{n\pi x}{b} - \frac{m\pi y}{a}\right\} - \cos\left\{\frac{n\pi x}{b} + \frac{m\pi y}{a}\right\}\right] \tag{3}$$

Similarly, we take a two-dimensional specimen and impulsively load it in tension T for all time.

$$X_x = \sum_m \sum_n \frac{2T(1-\cos m\pi)(\cos n\pi - 1)}{m\,n\pi^2}\cos\left(\frac{n\pi a_0 t}{b}\right) \left[\cos\left\{\frac{n\pi x}{b} - \frac{m\pi y}{a}\right\} - \cos\left\{\frac{n\pi x}{b} + \frac{m\pi y}{a}\right\}\right]$$

Just as in the one-dimensional case, failure occurs when the tension T exceeds one half of its static limit. Therefore, the coefficient relating the wave amplitude to the yield stress is

$$Q_{2D} \equiv 4/\pi^2 \tag{4}$$

The value of Q_{2D} is not restricted to a particular failure mode. The maximum tension T may be limited by either shear or tension. In obtaining Eq. (4), it was stated only that the impulsive load is twice as strong as the static load. The primary mode, whose amplitude is $8\ T/\pi^2$, will break when T is "½". Hence, Q_{2D} is $4/\pi^2$.

For an axial load such as that applied to the ice crystal, Mohr's circle[17] predicts that the maximum shear S occurs at

$$y = \pm x + \text{constant}$$

and is of strength

$$S = X_x/2$$

Examining Eq. (3), we see that the strength of the (m,n) mode is a maximum along

$$y = \pm (a/b)(n/m)x + \text{constant}$$

Therefore, the natural mode selection that would maximize the shear stress on the wave is

$$a/b \equiv m/n$$

Under the constraint of $b \geq a$, hence $n \geq m$, the shear stress on the two-dimensional ice crystal may be expressed as

$$S = \frac{-P_s(1-\cos m\pi)a}{m^2\pi^2 b}\cos\left(\frac{m\pi a_0 t}{a}\right)\left\{\cos\left[\frac{m\pi}{a}(x-y)\right] - \cos\left[\frac{m\pi}{a}(x+y)\right]\right\}$$

The dynamic fracture criterion predicts failure for the critical value of m, denoted by m_c. Equating the wave amplitude of S to $Q_{2D}S_s$,

$$\frac{2P_s a}{m_c^2\pi^2 b} = S_s Q_{2D} \quad \text{for} \quad (b \geq a)$$

the value of m_c becomes

$$m_c = \sqrt{\left(\frac{P_s}{2S_s}\right)\left(\frac{a}{b}\right)}, \quad \left(\frac{P_s}{2S_s} \geq \frac{b}{a}\right) \tag{5}$$

Note: for $m_c < 1$, we must use the one-dimensional results of Sec. II B, otherwise the lateral dimension of the fragment is greater than a. The results are continuous if it is assumed that the maximum axial stress is limited by the shear mode ($\sigma_s = 2S_s$). The characteristic fragment size is a/m_c or

$$\ell_{2D} = \sqrt{\left(\frac{2S_s}{P_s}\right)(ab)} \quad \text{for} \quad \left(\frac{P_s}{2S_s} \geq \frac{b}{a}\right) \text{ or } (\ell < a) \tag{6a}$$

and

$$\ell_{1D} = \left(\frac{\sigma_s}{P_s}\right)b \quad \text{for} \quad \left(\frac{P_s}{2S_s} \leq \frac{b}{a}\right) \text{or } (\ell > a) \tag{6b}$$

Hence, the two-dimensional shattering analysis is appropriate only if the fragment size is less than the small dimension of the initial crystal. Otherwise, shattering is one-dimensional along the length of the specimen.

E. Three-Dimensional Shattering

Suppose that we now have a three-dimensional crystal of length b and base area a^2 ($b \geq a$). Expanding the applied force in a triple Fourier series, the amplitude of the wave would be inversely proportional to the mode number cubed.

$$A_{n,m,q} \sim P_s/nmq$$

where

$$n/b = m/a = q/a$$

or

$$A_{n,m,q} \approx P_s a/m^3 b$$

Applying the dynamic fracture criterion to the amplitude of the wave, we obtain

$$P_s a/m_c^3 b \sim S_s$$

or

$$m_c \approx (P_s/S_s)^{1/3}(a/b)^{1/3}$$

The fragment size is a/m_c or

$$\ell_{3D} = \left(\frac{2S_s}{P_s}\right)^{1/3}(a^2 b)^{1/3} \quad \text{for} \quad \left(\frac{P_s}{2S_s} \geq \frac{b}{a}\right) \tag{7}$$

where the constant was chosen to be continuous with the one-dimensional results when $\ell_{3D} = a$. For $\ell_{3D} > a$, we again use the one-dimensional result [Eq. (6b)]. Hence, the three-dimensional analysis is appropriate only if the fragment size is less than a. Otherwise, shattering is one-dimensional along the length of the specimen.

III. Ice Crystal Breakup

A. Description of the Model

As the fractured ice crystal passes through the vehicle shock layer, it will break up and deform by the action of the shock-layer gas. The deformation of the fragment cloud is studied in Ref. 13. However, on a time scale small with respect to the cloud deformation time, ice crystal breakup must be assessed in order to determine the appropriate model for the fragment cloud. That is, does the fragment cloud behave as a separate fluid, a two-phase flow, or as a fluidized bed?

To begin to answer this question, we see from Sec. IIA that the maximum velocity imparted to the solid particle is

$$U_{\max} = \frac{a_0 A_k}{E} = \frac{a_0 P_s}{E}$$

Since $a_0 \sim 3$ km/sec, $E \sim 10^5$ atm, and $P_s \sim 10^3$ atm (max), we obtain

$$U_{\max} \sim 30 \text{m/sec}$$

The expansion Mach number (relative to the gas) corresponding to $U_{\max}$ would be 0.1 upstream of the vehicle shock and 0.01 downstream of the shock. Hence, the expansion is much too slow to be thought of as an "explosion." Rather, we think of it as a "convective separation" where the crystal fragments separate with some characteristic velocity indicative of the initial fracturing process. As the fragments separate, shock-layer gas will influx through the cracks as shown in Fig. 6. The time scale for gas to penetrate the fragment cloud is short compared to the time required for the fragment to respond dynamically to the gas. In fact, the latter time scale is the deformation time and this is the distinction between crystal breakup and cloud deformation.

As the gas penetrates through the cracks, the gas seeks pressure equilibrium ($\nabla P \to 0$). However, the pressure dif-

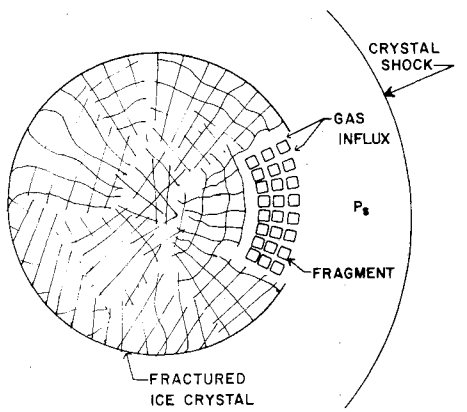

Fig. 6 Ice crystal breakup.

ference across a fragment is $\ell\nabla P$, which, if in excess of σ_s, will fracture the fragment. Continuous fracturing of the fragments would increase the surface/volume of the solid and prevent further influx of gas. If the incoming gas achieves pressure equilibrium within the fragment cloud before further fracturing can occur, the fragment cloud must be treated as a two-phase flow. However, if further fracturing prevents the gas from penetrating the fragment cloud, the cloud may be thought of as a separate gas which deforms in much the same way that a liquid drop deforms. In the following sections, it is shown that the fragment cloud may be treated as a separate fluid which deforms as a continuous medium.

B. Formulation of the Model

Investigating the stagnation region of the fragment cloud, we assume that the velocity of the fragments is radial with magnitude increasing linearly in r

$$U_r = (a_0 P_s/E)\,(r/R_0)$$

where R_0 is the initial radius of the fragment cloud or ice crystal. If the fragments expand without slowing down

$$r(t) = r(o)\left(1+\frac{a_0 P_s t}{E R_0}\right)$$

where $r(0)$ is the independent coordinate r and $r(t)$ is the coordinate of the fragment that was initially at r. The porous volume within the fragment cloud may be expressed as

$$V_p = \left(\frac{4}{3}\pi r^3(t) - \frac{4}{3}\pi r^3\right)\frac{\Omega}{4\pi}$$

where Ω is the solid angle subtended by the stagnation area. For $t \ll R_0/U_{\max}$,

$$V_p = \frac{\Omega a_0 P_s t}{E R_0} r^3 \tag{8a}$$

$$dV_p = A_p dr \tag{8b}$$

and

$$A_p = \frac{3\Omega a_0 P_s t r^2}{E R_0} \tag{8c}$$

The equations of motion for the gas are written using a control volume fixed to the fragments. It is assumed that the velocity of the fragments is constant in time and small with respect to the gas velocity.

Gas continuity

$$\frac{\partial}{\partial r}(\bar\rho \bar u A_p)\,dr = -\frac{\partial}{\partial t}(\bar\rho dV_p)$$

Gas momentum

$$\frac{\partial}{\partial t}(\bar\rho \bar u dV_p) + \frac{\partial}{\partial r}(\bar\rho \bar u^2 A_p)\,dr = -A_p\frac{\partial \bar p}{\partial r}dr - F dA_s - N dA_n$$

where $\bar\rho$ is the gas density, $\bar u$ the gas velocity, and $\bar p$ is the gas pressure. The shear force between the fragments and the gas is denoted by F. The cracks are not necessarily collinear. Hence, the presence of a fragment at the end of each crack would result in a stagnation pressure N, applied over the normal surface area, dA_n, as denoted in the preceding equation.

To determine F, consider the incompressible flow between parallel plates separated by distance $2h$

$$u = u_{\ell}\,(h^2 - y^2)/h^2$$

where y is measured from the centerline, equidistant between the plates. The average gas velocity $\bar u$ is related to u_{ℓ} by continuity

$$\bar u = \int_{-h}^{h} u\left(\frac{dy}{2h}\right) = 2u_{\ell}/3$$

The shear stress F is determined from

$$F = \bar\mu \frac{\partial u}{\partial y}\bigg|_{-h} = \frac{2u_{\ell}\bar\mu}{h} = \frac{3\bar u\bar\mu}{h}$$

where $\bar\mu$ is the gas viscosity.

To determine $h(r,t)$, note that the porous volume per fragment is $6h\ell^2$ where ℓ is the fragment size. The number of fragments in volume element $\Omega r^2 dr$ is $\Omega r^2 dr/\ell^3$. Therefore, the porous volume element is

$$dV_p = \left(6h\ell^2\right)\left(\frac{\Omega r^2 dr}{\ell^3}\right)$$

Comparing to Eq. (8), we obtain h.

$$h = \frac{a_0 P_s \ell t}{2E R_0}$$

The surface area of each fragment is $6\ell^2$. Thus, the net surface area in volume element $\Omega r^2 dr$ is

$$dA_s = 6\ell^2\left(\frac{\Omega r^2 dr}{\ell^3}\right)$$

and

$$F dA_s = \frac{36\bar\mu\bar u E R_0 \Omega r^2 dr}{\ell^2 a_0 P_s t}$$

The normal pressure force N is

$$N = (\bar\rho \bar u^2/2)\ \operatorname{sign}(\bar u)$$

The normal surface area associated with each fragment is $2h\ell$. Thus,

$$dA_n = 2h\ell\left(\frac{\Omega r^2 dr}{\ell^3}\right)$$

or

$$N dA_n = \frac{a_0 P_s t \bar\rho \bar u^2 \operatorname{sign}(\bar u)\,\Omega r^2 dr}{2E R_0 \ell}$$

Using V_p, A_p, $F dA_s$, and $N dA_n$, the continuity and momentum equations become, respectively,

$$\frac{t}{r^2}\frac{\partial}{\partial r}(\bar\rho \bar u r^2) + \frac{\partial}{\partial t}(t\bar\rho) = 0 \tag{9}$$

and

$$\bar\rho\frac{\partial \bar u}{\partial t} + \bar\rho\bar u\frac{\partial \bar u}{\partial r} + \frac{\partial \bar p}{\partial r} + \frac{12\,\bar u\bar\mu E^2 R_0{}^2}{a_0{}^2 P_s{}^2 \ell^2 t^2} + \frac{\bar\rho \bar u^2}{6\ell}\operatorname{sign}(\bar u) = 0 \tag{10}$$

The fragment size ℓ appearing in Eq. (10) is a time-dependent quantity which is yet to be determined. If we apply a pressure gradient across a crystal fragment, that fragment will fracture when

$$\ell\frac{\partial \bar p}{\partial r} > \sigma_s$$

The shattering theory indicates that the fragment will break into smaller fragments of size $(\sigma_s/\ell\partial\bar{p}/\partial r)^{1/3}\ell$ in a time scale of order ℓ/a_0. Therefore

$$\frac{D\ell}{Dt} \doteq \frac{\partial\ell}{\partial t} = -\left\{\frac{\ell-[\sigma_s/\ell(\partial\bar{p}/\partial r)]^{1/3}\ell}{(\ell/a_0)}\right\}$$

or

$$\frac{\partial\ell}{\partial t} = -a_0\left\{1-[\sigma_s/\ell(\partial\bar{p}/\partial r)]^{1/3}\right\} \tag{11}$$

Equations (9-11) represent three equations in the four unknowns $\bar{\rho}$, $\bar{u}$, $\bar{p}$, and ℓ. In the next two sections, they are solved by specifying $\bar{\rho}$ in the incompressible and sonic limits.

C. Incompressible Solution

In the incompressible limit, the continuity equation yields $\bar{u}$,

$$\bar{u} = -r/3t$$

and the momentum equation yields $\bar{p}\ (\ell,r,t)$

$$\frac{\partial\bar{p}}{\partial r} = \frac{4\bar{\mu}E^2R_0{}^2r}{a_0{}^2P_s^2\ell^2t^3} - \frac{4\bar{\rho}r}{9t^2} + \frac{\bar{\rho}r^2}{54\ell t^2} \tag{12}$$

Substituting $\partial\bar{p}/\partial r$ into the shattering relation, Eq. (11), yields

$$\frac{\partial(\ell/\ell_0)}{\partial\tau} = -1+\left[\frac{\epsilon_0{}^3\left(\frac{r}{R_0}\right)}{\left(\frac{\ell}{\ell_0}\right)\tau^3} + \frac{\epsilon_1{}^3\left(\frac{r}{R_0}\right)^2}{\tau^2} - K^3\epsilon_1{}^3\frac{\left(\frac{\ell}{\ell_0}\right)\left(\frac{r}{R_0}\right)}{\tau^2}\right]^{-1/3} \tag{13}$$

where

$$\ell_0 = (\sigma_s/P_s)^{1/3}R_0$$

$$\tau = t/(\ell_0/a_0)$$

$$Rey = \bar{\rho}a_0R_0/\bar{\mu}$$

$$\epsilon_0 = \left(\frac{4\bar{\rho}}{\rho}\right)^{1/3}\left(\frac{1}{Rey}\right)^{1/3}\left(\frac{E}{P_s}\right)^{2/9}\left(\frac{E}{\sigma_s}\right)^{7/9}$$

$$\epsilon_1 = [(\bar{\rho}/\rho)^{1/3}P_s{}^{2/9}E^{1/3}]/[(54)^{1/3}(\sigma_s)^{5/9}]$$

$$K = (24)^{1/3}(\sigma_s/P_s)^{1/9}$$

For the ice crystal/shock-layer interaction problem, we are interested in the following range of values

$$Rey = 10^4 \text{ to } 10^5$$

$$P_s = 10 \text{ atm to } 10^3 \text{ atm}$$

$$\sigma_s \doteq 10 \text{ atm}$$

$$\rho \doteq 100\,\bar{\rho}$$

$$E \doteq 10^5 \text{ atm}$$

Figure 7 illustrates that our range of interest (cross-hatched region) lies in the domain where $\epsilon_0 \gg \epsilon_1$, $\epsilon_0 \gg K\epsilon_1$, and $\epsilon_0 \gg 1$.

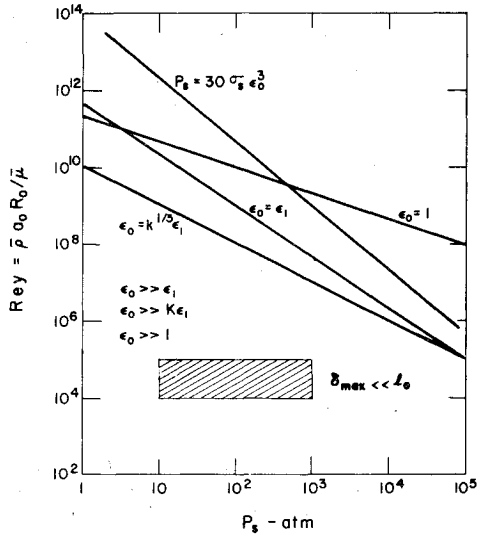

Fig. 7 Ordering of the shattering equation (incompressible flow).

Thus, for r near R_0, Eq. (13) becomes

$$\frac{\partial(\ell/\ell_0)}{\partial\tau} = -1+\frac{(\ell/\ell_0)^{1/3}\tau}{\epsilon_0} \tag{14}$$

The nature of Eq. (14) depends on the size of ϵ_0. For $\epsilon_0 \ll 1$, shattering will stop at some value of ℓ near ℓ_0 (shattering stops when $\partial\ell/\partial\tau = 0$ or when $\ell = 0$). However, for the case of interest ($\epsilon_0 \gg 1$) the approximate solution to (14) is

$$\ell/\ell_0 \doteq 1-\tau \tag{15}$$

for $\tau \leq 1$ ($\ell = 0$ for $\tau \geq 1$). Thus, continuous shattering at $r = R_0$ breaks the outer fragments into tiny fragments which will prevent further penetration by the shock-layer gas.

To estimate the penetration distance of the shock-layer gas, we assume that the pressure gradient at $r = R_0$ is continuous over the penetration distance, δ

$$\delta = P_s/(\partial\bar{p}/\partial r) \quad \text{for } \delta_{max} \ll R_0 \tag{16}$$

From Eqs. (15) and (12), the pressure gradient is expressed in terms of dimensionless parameters previously defined.

$$\frac{\partial\bar{p}}{\partial r} = \frac{\epsilon_0{}^3\sigma_s}{\ell_0\tau^3(1-\tau)^2}$$

The penetration distance becomes

$$\frac{\delta}{\ell_0} = \frac{P_s\tau^3(1-\tau)^2}{\epsilon_0{}^3\sigma_s}$$

or

$$\frac{\delta_{max}}{\ell_0} \doteq \frac{P_s}{30\sigma_s\epsilon_0{}^3}$$

For the range of parameters illustrated in Fig. 7, δ_{max} is much less than ℓ_0. Thus, the shock-layer gas does not penetrate the fragment cloud, and the fragment cloud may be treated as a separate gas or incompressible fluid without surface tension.

D. Sonic Solution

The gas flux into the porous regions of the fragment cloud is more likely to be sonic than incompressible. Rewriting the

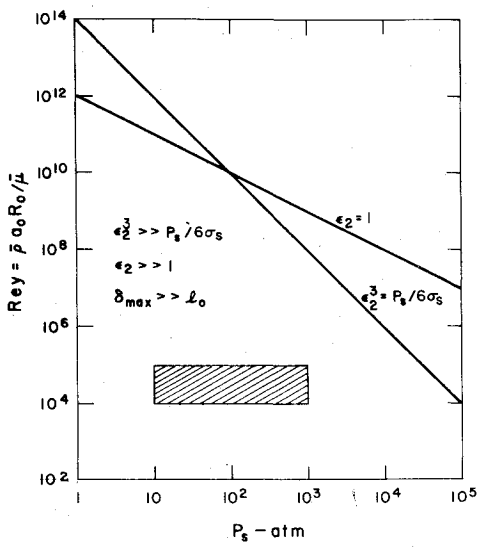

Fig. 8 Ordering of the shattering equation (sonic flow).

shattering equation for $\bar{u}=\bar{u}^*$, we obtain

$$\frac{\partial(\ell/\ell_0)}{\partial\tau} = -1+\left[\frac{{\epsilon_2}^3}{(\ell/\ell_0)\tau^2}+\frac{P_s}{6\sigma_s}\right]^{-1/3} \tag{17}$$

where we assumed

$$\bar{\rho}\bar{u}^*\bar{u}^* = P_s$$

and

$$\epsilon_2 = \left(\frac{12}{Rey}\right)^{1/3}\left(\frac{\bar{u}^*}{a_0}\right)^{1/3}\left(\frac{\bar{\rho}}{\rho}\right)^{1/3}\frac{E}{\sigma_s^{2/3}P_s^{1/3}}$$

For $\bar{u}^*=a_0$ and the range of parameters indicated in Sec. IIIC, Fig. 8 illustrates that the ϵ_2^3 terms in Eq. (17) is dominant.

$$\frac{\partial(\ell/\ell_0)}{\partial\tau} \doteqdot -1+\frac{(\ell/\ell_0)^{1/3}\tau^{2/3}}{\epsilon_2}$$

For $\epsilon_2 \gg 1$, $\ell/\ell_0 \doteqdot 1-\tau$ and the pressure gradient is expressed as

$$\frac{\partial\bar{p}}{\partial r} = \frac{{\epsilon_2}^3\sigma_s}{\ell_0\tau^2(1-\tau)^2} \tag{18}$$

The penetration depth of the shock-layer gas is determined from Eqs. (16) and (18)

$$\frac{\delta}{\ell_0} = \frac{P_s\tau^2(1-\tau)^2}{{\epsilon_2}^3\sigma_s}$$

or

$$\frac{\delta_{max}}{\ell_0} = \frac{P_s}{16{\epsilon_2}^3\sigma_s}$$

For the range of parameters indicated in Fig. 8, $\delta_{max} \ll \ell_0$. The shock-layer gas does not penetrate the fragment cloud and the fragment cloud may be treated as a separate gas or incompressible fluid without surface tension.

IV. Conclusions

The shattering of ice crystals in the shock layer of a hypersonic vehicle has been studied theoretically. A dynamic fracture criterion, which is subject to experimental verification, has been developed to determine the size and velocity of the crystal fragments. Using the initial fragment size and velocity from the model for dynamic fracture, it has been concluded that the outer fragments continue to fracture and prevent the shock-layer gas from penetrating the fragment cloud. Thus, the fragment cloud may be treated as a separate incompressible fluid or liquid drop. This basic conclusion is a consequence of the model for ice crystal breakup and is only weakly dependent upon the actual shattering process. Hence, the dynamic fracture criterion need only be qualitatively correct in order to support the conclusion that shattered ice crystals can be treated as liquid drops.

The dynamics of the deformable drops have been modeled elsewhere.[13] The flattening of the fragment cloud increases the drag area of the ice crystal and reduces its impact velocity at the vehicle. Hence, the fracturing of the ice crystal at the vehicle shock may significantly reduce the erosion of the vehicle.

References

[1] Probstein, R. F. and Fassio, F., "Dusty Hypersonic Flows," *AIAA Journal*, Vol. 8, April 1970, pp. 772-779.

[2] Engel, O. G., "Fragmentation of Waterdrops in the Zone Behind an Air Shock," *Journal of Research of the NBS*, Vol. 60, March 1958, pp. 245-280.

[3] Hanson, A., Domich, E., and Adams, H., "Shock Tube Investigation of the Breakup of Drops by Air Blasts," *The Physics of Fluids*, Vol. 6, Aug. 1963, pp. 1070-1080.

[4] Ranger, A. A. and Nicholls, J. A., "Aerodynamic Shattering of Liquid Drops," *AIAA Journal*, Vol. 7, Feb. 1969, pp. 285-290.

[5] Reinecke, W. and Waldman, G., "An Investigation of Water Drop Disintegration in the Region Behind Strong Shock Waves," *Proceedings of the Third International Conference on Rain Erosion and Related Phenomena*, Aug. 1970, Hartley Whitney, Hampshire, England.

[6] Waldman, G. D. and Reinecke, W. G., "Particle Trajectories, Heating, and Breakup in Hypersonic Shock Layers," *AIAA Journal*, Vol. 9, June 1971, pp. 1040-1048.

[7] Harper, E. Y., Grube, G. W., and Chang, I-Dee, "On the Breakup of Accelerating Liquid Drops," *Journal of Fluid Mechanics*, Vol. 52, Pt. 3, 1972, pp. 565-591.

[8] Simpkins, P. G. and Bales, E. L., "Water-Drop Response to Sudden Accelerations," *Journal of Fluid Mechanics*, Vol. 55, Pt. 4, 1972, pp. 629-639.

[9] Waldman, G. D., Reinecke, W. G., and Glenn, D. C., "Raindrop Breakup in the Shock Layer of a High-Speed Vehicle," *AIAA Journal*, Vol. 10, Sept. 1972, pp. 1200-1204.

[10] Jaffe, N. A., "Droplet Dynamics in a Hypersonic Shock Layer," *AIAA Journal*, Vol. 11, Nov. 1973, pp. 1562-1564.

[11] Reinecke, W. G. and Waldman, G. D., "Shock Layer Shattering of Cloud Drops in Reentry Flight," AIAA Paper 75-152, Pasadena, Calif., 1975.

[12] Finson, M. L., Lewis, P. F., Wu, P. K. S., Teare, J. D., Pirri, A. N., and Nebolsine, P. E., "Advanced Reentry Aeromechanics, Interim Scientific Report," PSI TR-10, Aug. 1974, Physical Sciences Inc.

[13] Simons, G. A., "Liquid Drop Acceleration and Deformation," *AIAA Journal*, Vol. 14, Feb. 1976, pp. 278-280.

[14] Rakhmatulin, KH. A. and Dem'Yanov, YU. A., *Strength under High Transient Loads*, 1961, edited by S. Monson, Jerusalem and Wiener Bindery Ltd., Jerusalem, 1966, p. 81.

[15] Singer, F. L., *Strength of Materials*, 2nd ed., Harper & Brothers, New York, 1962, p. 471.

[16] Kittel, C., *Introduction to Solid State Physics*, 3rd ed., Wiley, New York, 1966, Ch. 5.

[17] Perry, D. J., *Aircraft Structures*, McGraw-Hill, New York, 1950, pp. 88-96.